FEBS *Letters*

Review

Spatially distributed cell signalling

Boris N. Kholodenko *

Systems Biology Ireland, University College Dublin, Belfield, Dublin 4, Ireland
Department of Pathology, Anatomy and Cell Biology, Thomas Jefferson University, Philadelphia, PA 19107, USA

A R T I C L E   I N F O

A B S T R A C T

Emerging evidence indicates that complex spatial gradients and (micro)domains of signalling activities arise from distinct cellular localization of opposing enzymes, such as a kinase and phosphatase, in signal transduction cascades. Often, an interacting, active form of a target protein has a lower diffusivity than an inactive form, and this leads to spatial gradients of the protein abundance in the cytoplasm. A spatially distributed signalling cascade can create step-like activation profiles, which decay at successive distances from the cell surface, assigning digital positional information to different regions in the cell. Feedback and feedforward network motifs control activity patterns, allowing signalling networks to serve as cellular devices for spatial computations.
© 2009 Federation of European Biochemical Societies. Published by Elsevier B.V. All rights reserved.

1. Introduction

Not long ago, a cell was viewed as a "bag" of enzymes that resembled an enzymologist's test tube. Since then, it became clear that enzymatic pathways are spatially organized within a cell. Enzymes can associate with each other and various cellular structures, such as internal membranes and cytoskeleton. Reaction products can directly be transferred between enzymes without equilibrating with the bulk phase, a phenomenon referred to as metabolic channelling [1–3]. Likewise, the spatial signal propagation was traditionally considered between cells, usually in the context of morphogenesis. However, recent discoveries have changed our perception of cell signalling [4]. A new view is emerging that pivotal cellular processes, including proliferation and motility, critically depend on the spatial features of intracellular signals, which propagate positional information and encode precise membrane, cytoplasmic, or nuclear location of the components of signalling cascades [5,6].

More than 50 years ago, seminal Turing's work showed that a break of the spatial symmetry and formation of periodic concentration patterns can occur in homogeneous media through reaction–diffusion processes [7]. This and subsequent work laid the foundation of the chemical–physical theory of morphogenesis. If two morphogens, commonly referred to as activator and inhibitor, have different diffusivities, and the activator switches on the inhibitor, then the spatially uniform distribution is unstable, and this

instability drives the formation of heterogeneous spatial patterns [7]. However, precisely such conditions can rarely be found in developmental systems, and many experimental biologists prefer explaining the embryonic pattern formation by specific gene regulatory mechanisms, rather than by the dynamics of reactions and diffusion. Although the Turing mechanism has successfully been exploited to account for patterns of repeated stripes and spots on the skin of many animal species, direct molecular evidence remains scarce [8].

In living cells, signalling pathways are highly spatially organized, and often activator and deactivator enzymes localize to distinct cellular structures. For instance, activating signals can occur on the plasma membrane or intracellular membranes where activated receptors and small G-proteins, such as Ras, reside, whereas inactivating processes can be distributed throughout the cytoplasm. In other words, intracellular environment for reactions and diffusion is initially inhomogeneous and does not resemble the uniform media considered in Turing models. For a protein phosphorylated by a membrane-bound kinase and dephosphorylated by a cytosolic phosphatase, Brown and Kholodenko predicted that there can be a gradient of the phosphorylated form, high close to the membrane and low within the cell [9]. This spatial phosphoprotein pattern is stable and depends on the pre-existing separation of antagonistic enzymes brought about by the spatial organization of a cell.

In this mini-review, I survey spatial aspects of intracellular signalling. Computational modelling and systems analysis allow linking the knowledge of molecular mechanisms to complex spatiotemporal dynamics of signal transduction within a cell.

* Fax: +1 353 1 716 6713.
E-mail address: Boris.Kholodenko@ucd.ie

High-resolution microscopic techniques, including single-molecule imaging, help visualize the distribution of signalling proteins and their activities in space and time. I demonstrate how both theoretical studies and experimental work have synergistically increased our understanding of spatial control of cell signalling.

2. Spatial gradients of signalling activities in post-translational modification cycles

The fundamental language of cell signalling is reversible covalent modification of cellular proteins, which occurs in response to external and internal cues. In eukaryotes, post-translational protein modification reactions include phosphorylation of Tyr, Thr and Ser residues, methylation of Arg and Lys, acetylation, ubiquitylation and sumoylation of Lys, and other modifications [10]. All these modifications dramatically change protein activities, generating universal motifs of cell signalling: cycles formed by two or more interconvertible forms of a signalling protein, which is modified by two opposing enzymes [11]. Such enzymes can be a kinase and a phosphatase, or the corresponding enzyme pairs for methylation, acetylation or ubiquitylation. An important variation to this theme is the exchange of guanine nucleotides GDP and GTP on small G-proteins, such as proteins of the Ras and Rho families. A GTP-bound form of a small G-protein is usually active, whereas a GDP-bound form is inactive. The two opposing enzymes catalyzing this modification cycle are a guanine nucleotide exchange factor (GEF) and a GTP-hydrolysis activating protein (GAP).

A well-known property of protein modification cycles is "ultrasensitivity" to input signals, which occurs when the converting enzymes operate near saturation [12]. Depending on the degree of saturation, the response of either interconvertible form ranges from a merely hyperbolic to an extremely steep sigmoid curve. Sequestration of a signalling protein by converting enzymes significantly decreases sigmoidicity of responses [13]. If an activating enzyme and a deactivating enzyme (two opposing enzymes) are separated in the space, the steady-state activity gradients of the target protein will occur in a cell [9]. The kinetic properties of such cycles, where the opposing enzymes are spatially segregated, significantly differ from the properties of cycles with uniformly distributed enzymes. For instance, the dose–response curves strongly depend on the diffusivity of the target protein and generally become less ultrasensitive [14].

We consider a universal protein modification cycle where an activator is confined to a membrane or cellular structure, such as chromatin, and a deactivator is distributed in the cytoplasm. Provided that the deactivator kinetics is far from saturation, the concentration profile of the active fraction of the target protein decays almost exponentially with the distance from the activator location (Fig. 1, black line). The characteristic decay length of the gradient (L_{grad}) is controlled by the protein diffusivity (D) and the apparent first-order rate constant of the deactivator ($k_{deact} = V_{max}/K_M$, where V_{max} and K_M are the maximal rate and Michaelis constant of the deactivation reaction, respectively). Importantly, L_{grad} does not depend on the activator kinetics, and it is expressed as follows [9],

$$L_{grad} = \sqrt{D/k_{deact}}. \tag{1}$$

Recent advances in the fluorescence resonance energy transfer-based technologies enabled experimental discoveries of intracellular activity gradients in live cells. Such gradients of active protein forms were reported for the small GTPase Ran [15], phosphorylated stathmin oncoprotein 18 [16], the yeast mitogen activated protein kinase (MAPK) Fus3 [17], and Aurora B kinase [18]. Notably, all these gradients are brought about by the spatial separation of opposing enzymes in activation–deactivation cycles of protein
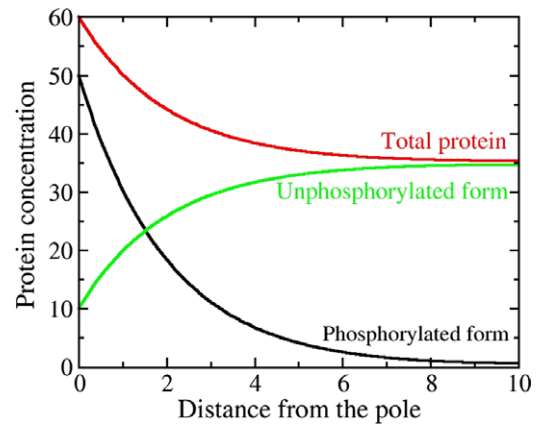

Fig. 1. Spatial gradients in a cylindrical cell with the kinase located at the left pole and cytoplasmic phosphatase. When the phosphatase is far from saturation, the concentration profile $C_p(x)$ of the phosphorylated form (black line) is calculated using a simple analytical expression presented in Ref. [32], $C_p(x) = C_p(0)\left(\frac{e^{x/L_{grad}} + e^{2L/L_{grad}} e^{-x/L_{grad}}}{1 + e^{2L/L_{grad}}}\right)$, where the characteristic decay length of the gradient (L_{grad}) is given in Eq. (1), and x is the distance from the pole. The concentration $C(x)$ of the unphosphorylated form (green line) and the total protein abundance (red line) are calculated using Eqs. (6) and (7) where the ratio of diffusivities D/D^* was assumed 2. The cell length $L = 10$ μm, $L_{grad} = 2$ μm, $C_p(0) = 50$ nM, $C(0) = 10$ nM.

modification, but not by the spatial symmetry breaking and formation of periodic spatial patterns, as it occurs in the Turing mechanism.

3. Spatial gradients of total protein abundances

3.1. Different diffusivities result in the intracellular gradients of protein abundances

There are many cases in which active and inactive protein forms may have different diffusivities. For instance, the active form of a signalling protein often interacts with other proteins, generating multi-protein complexes. The diffusivity of a molecule or a complex, D, is determined by the Einstein–Stokes equation, $D = k_B T/6\pi\eta S$, where k_B is Boltzmann's constant, T is the absolute temperature, η is the viscosity of the medium, and S is the Stokes radius, which is roughly proportional to the cube root of the molecular weight (MW). Therefore, when an active form of a low MW protein associates with a high MW protein, or forms a multi-protein complex, the Stokes radius of the complex can be much larger than the Stokes radius of an inactive form. Consequently, the diffusivity of the complex can be considerably less than the diffusivity of the inactive form. Provided that the complex is sufficiently stable, this leads to a significant decrease in the apparent diffusivity of the active protein form.

Likewise, suppose that the active form (A^*) of a signalling protein binds to an immobile buffer (B), whereas the inactive form (A) does not, and that the diffusivities of the free forms A and A^* are the same (D). Diffusion and binding of A^* to the buffer is described by the standard reaction–diffusion equations,

$$\frac{\partial [A^*]}{\partial t} = D\Delta[A^*] - k_a[A^*] \cdot [B] + k_d[A^*B], \tag{2}$$

$$\frac{\partial [A^*B]}{\partial t} = k_a[A^*] \cdot [B] - k_d[A^*B]. \tag{3}$$

Here k_a and k_d are the association and dissociation rate constants, $[B]$ and $[A^*B]$ are the concentrations of the free and bound forms of the immobile buffer (since these forms are immobile there is no diffusion term in Eq. (3)). Assuming that the binding reaction

is in rapid equilibrium and the total buffer concentration (B^{total}) is much larger than the total concentration of the active form, the concentration of the bound fraction can be expressed in terms of the equilibrium dissociation constant ($K_d = k_d/k_a$) and the total buffer concentration $[B^{total}]$,

$$[A^*B] \approx \frac{k_a}{k_d}[A^*] \cdot [B^{total}] = \frac{[A^*] \cdot [B^{total}]}{K_d}. \tag{4}$$

Summing Eqs. (2) and (3) and using Eq. (4), we find that diffusion of the active form A^* can be described using the apparent diffusivity D^* as follows [19,20]:

$$\frac{\partial [A^*]}{\partial t} = D^* \Delta [A^*], \quad D^* = \frac{D}{1 + [B^{total}]/K_d}. \tag{5}$$

Thus for $[B^{total}]/K_d \geqslant 1$, the apparent diffusivity of the active form differs dramatically from the diffusivity of the inactive form, which does not bind to the buffer.

When diffusivities of active and inactive protein forms are equal, the total concentration of the target protein is the same in any location. The gradients generated by the two forms are equal and have opposite signs [9]. However, for different diffusivities, this is no longer valid. For illustrative purposes, we consider the simplest one-dimensional geometry that corresponds to a cylindrical bacterial cell, but all results apply to a spherically symmetrical cell in three dimensions. We assume that an activator, e.g., a kinase, is localized to the membrane at one pole of this cell and a deactivator phosphatase is distributed in the cytoplasm. We define the gradient of the phosphorylated form ($Grad_p$), as the difference between the high concentration of that form at the pole and the lower concentration in the cytoplasm, at a distance from the pole. For the unphosphorylated, inactive form, the direction of the gradient is opposite, so that the gradient of the unphosphorylated form ($Grad_u$) is defined as the difference between the higher concentration at a distance from the pole and the lower concentration at the pole. Remarkably, for any feasible phosphatase kinetics (e.g., regardless of whether the phosphatase is far or close to saturation), the ratio of these gradients is inversely proportional to the ratio of the diffusivities of the phosphorylated and unphosphorylated forms [21],

$$Grad_p/Grad_u = D/D^* \geqslant 1. \tag{6}$$

Since the diffusivity D of the inactive form is higher than the apparent diffusivity D^* of the active form, we conclude that the phosphoprotein gradient is higher than the gradient of the inactive form. Consequently, the gradient of the total protein abundance $Grad_{total}$, which is defined as the difference between the protein abundance near the pole and in the cytoplasm, occurs due to the more precipitous gradient of the phosphorylated form,

$$Grad_{total} = (1 - D^*/D)Grad_p. \tag{7}$$

Fig. 1 illustrates how the difference in the diffusivities of active and inactive protein forms brings about the spatial gradient of the protein abundance within a cell.

Experimental data obtained using high-resolution, single-molecule imaging techniques demonstrate that when two receptor monomers form a dimer, its diffusivity is much lower than predicted by the Einstein–Stokes equation for a doubling of the particle weight [22]. The fluid mosaic model of the cell membrane that was proposed by Singer and Nicolson [23] almost 40 years ago cannot explain such large decreases of diffusion coefficient upon receptor oligomerization. Advances in single-molecule imaging techniques have shown that in live cells the fluid mosaic model should be substituted by a model where the membrane is partitioned into small, dynamic subcompartments, called confinement zones or corrals [22]. It was proposed that a significant decrease

in the apparent diffusivity of a complex is explained by non-Brownian, confined diffusion in the membrane that contains corral-like barriers (fences) that restrict diffusion of oligomer complexes [24]. Recently, Monte Carlo techniques were employed to simulate the effect of spatial heterogeneities, microdomains and corrals, on the diffusion of molecules in the cell membrane [25,26]. For the certain ratios of the transition probabilities for diffusion across a boundary and within a corral, stochastic Monte Carlo simulations that used the lattice model of the membrane reproduced the effects of membrane "fences" and showed the diffusivities similar to those obtained experimentally [27,28].

4. Spatially distributed signalling cascades

Cascades of protein modification cycles form the backbone of major cellular signalling pathways that propagate external stimuli from the membrane to the nucleus or other distant targets. The spatial behaviour of signalling cascades has been studied in much less detail than their temporal activation dynamics [29]. For instance, we currently lack sufficient experimental insights into the generation of positional information during the propagation of external cues through protein modification cascades [30]. Typically, a plasma membrane receptor is stimulated by extracellular cues, and it then activates a kinase at the first cascade level in the vicinity of the membrane (Fig. 2A). The active kinase phosphorylates a kinase at the next level down the cascade, and this scenario is repeated at every downstream level. At each cascade level, the kinase is dephosphorylated by a cytoplasmic phosphatase. Since phosphorylation of the first kinase occurs only at the cell membrane, the phosphorylated fraction of this kinase that diffuses in the cell and becomes dephosphorylated decreases quickly towards the cell interior. How can the phosphorylation signal that was initiated at the plasma membrane propagate through the cytoplasm where it is terminated by phosphatases? In a recent paper, Munoz-Garcia et al. have shown the conditions under which signals that emanate from the membrane stall in the space (generating the precipitous gradients near the membrane), or robustly propagate through spatially distributed signalling cascades [31].

4.1. Generation of spatial stationary patterns by signalling cascades

For simplicity, we assume that in a cascade both kinases and phosphatases are far from saturation, and that the apparent first-order rate constants of kinases ($k_{act} = V_{max}^{kin}/K_M^{kin}$) and phosphatases ($k_{deact} = V_{max}^{phosph}/K_M^{phosph}$) are the same at the different cascade levels (note that the kinase maximal rates V_{max}^{kin} are parameters, proportional to the kinase abundances, whereas the actual rate is proportional to the phosphorylated kinase fraction at each space point). The ratio $\gamma = k_{deact}/k_{act}$ of the deactivator and activator activities is shown to be a key parameter that determines the signal propagation threshold [31], whereas $L_{grad} = \sqrt{D/k_{deact}}$ defines the characteristic length scale of the gradient for the first kinase activity [9]. The spatial profiles shown in Fig. 2B demonstrate that for small γ values, the phosphorylation signal carried by phosphorylated kinases at consecutive levels spreads increasingly from the membrane towards the cell centre. This can be a reason why cascades exist [32]. If $\gamma > 1$, the phosphorylation signal cannot propagate into a cell, and the profiles of activated kinases rapidly decay, reversing the signal back to the membrane (Fig. 2C). When γ is significantly less than one, the kinase activation profiles have long, flat plateaus, which abruptly decay at successive spatial locations (Fig. 2B). These step-like profiles generate spatial patterns that assign digital positional information to different regions in the cell. The maximal signalling amplitude, which is the active kinase fraction (the concentration of phosphorylated kinase divided by the
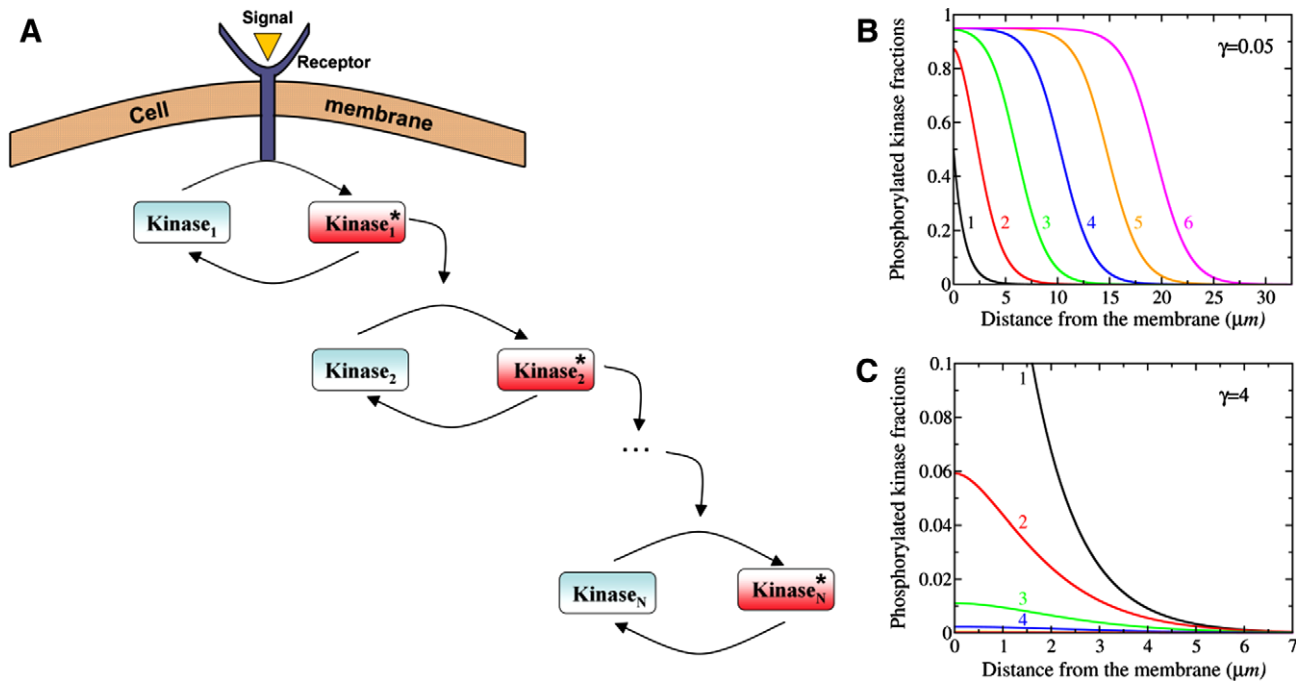
Fig. 2. Spatial propagation of phosphorylation signals and generation of positional information by protein modification cascades. (A) Diagram of a multi-level kinase cascade. Asterisks show phosphorylated, active forms of kinases. (B) Spatial patterns formed by consecutive activation profiles for small ratios of phosphatase and kinase activities ($\gamma = 0.05$), numbers indicate the cascade levels. (C) Rapid decay of signal propagation for large ratios of phosphatase and kinase activities ($\gamma = 4$). For details see Ref. [31].

total abundance of that kinase), can reach $(1 - \gamma)$. The spatial step size between consecutive decays of kinase activation for successive cascade layers is almost constant and equal to $\ln(1/\gamma)L_{grad}$ [31]. Digital information created by abruptly decaying activities at different distances from the cell membrane can be exploited by other cellular processes.

More complicated steady-state patterns of protein activities occur in cascades where active proteins at different levels can influence not only the immediate downstream level, but also other cascade levels. Known examples of such cascades include cascades of small G-proteins, such as the Rho-family GTPase cascades [33]. Here, we illustrate the appearance of intricate spatial profiles by considering a signalling cascade, where a GTPase at each cascade level positively or negatively influences GEFs or GAPs for GTPases at downstream levels [21]. The initial spatial heterogeneity occurs, because GTPase$_1$ at the first level is activated by GEF$_1$ that is localized at the membrane, whereas at downstream levels all GAPs (GTPase deactivators) and GEFs (activators) are freely diffusible. Similarly as above, the first GTPase$_1$ activity decreases almost exponentially in the cell interior [9]. If this GTPase$_1$ activates the deactivator GAP$_2$ at the second level, the GTPase$_2$ activity at the second level will *increase* with the distance from the membrane, because the corresponding GAP$_2$ activity exponentially decreases in the cell cytoplasm. Thus, this cascade level operates as a signal inverter in the space [21]. If we assume that GAP$_3$ at the third-level is activated by GTPases at the first and second levels, then the sum of two different signals, one of which decreases (active GTPase$_1$), but the other increases (active GTPase$_2$), can result in the *non-monotonic* GTPase$_3$ activity profile, which has a peak in the cell interior. In fact, complex, non-monotonic steady-state concentration profiles were recently reported for reaction cascades that regulate microtubule stabilization [34]. More intricate spatial gradients can be observed, when the components of a GTPase cascade localize to different subcellular components. If the activating (or deactivating) enzyme is located at both the plasma membrane and a structure within a cell, the resulting stationary gradients will

have sharp peaks (or deeps), so that the localization of these enzymes (signals) can be sensed by a cell. The aspects of complicated spatial activity patterns, which were briefly discussed, imply that GTPase networks may serve as devices for spatial computation inside living cells [21].

5. Intracellular domains of different protein activities

5.1. Spatial control of signalling by the cell shape and size

Living cells have diverse sizes and shapes and different surface-to-volume ratios. Moreover, the surface-to-volume ratio changes during many physiological processes, including cell growth. As mentioned above, activation signals are often generated at the plasma membrane by G-protein coupled receptors, membrane-bound kinases and GEFs, whereas deactivators terminate these signals in the cytoplasm. When a cell grows in size, the surface volume ratio decreases, and signalling messengers, such as phosphorylated proteins and activated GTPases, have to diffuse over larger distances from the membrane into the cytoplasm to reach their targets. As a result, active messengers are becoming progressively deactivated towards the cell interior [35]. Conversely, when a cell spreads over the substrate and flattens, the ratio of the plasma membrane surface area to the cell volume increases, and phosphoproteins become phosphorylated globally in the cell. In addition to these global effects, signalling pathways can be locally activated and deactivated in different parts of a cell, which have different geometry, such as the leading edge and trailing edge of migrating cells and neuron axon, dendrites and soma [6,35]. The lamellipodia and filopodia at the leading edge are much thinner than the cell body and trailing edge. It was shown both theoretically and experimentally that the GTPase Cdc42 is preferentially activated at the leading edge in extending protrusions, where the surface-to-volume ratio is larger than at the trailing edge [35,36].

5.2. Spatial control of signalling by feedforward and feedback network motifs

Spatial separation of the local activating and deactivating reactions can lead to the formation of intracellular domains of different protein activates [37]. In hippocampal neurons, the β-adrenergic receptor (β-AR) initiates the signalling cascade that activates the extracellular signal-regulated kinase (ERK) in the Raf/MEK/ERK (MAPK) pathway. The series of biochemical processes, initiated by β-AR, includes receptor-induced activation of adenylyl cyclase (AC), which leads to the cAMP synthesis and subsequent activation of the cyclic AMP-dependent protein kinase A (PKA). In turn, PKA activates the kinase B-Raf, which phosphorylates MEK (the ERK kinase), leading to ERK activation. Because AC is bound to the plasma membrane, whereas its opposing enzyme phosphodiesterase (PDE4) that degrades cAMP is soluble, intracellular gradients of the cAMP concentration can arise. In fact, the existence of cAMP gradients and localized microdomains was shown both theoretically and experimentally [38,39].

The cAMP/PKA-induced Raf/MEK/ERK cascade involves a negative feedback loop that is generated by PKA activation of PDE4 (cAMP deactivator), and a positive feedforward loop whereby PKA inhibits the phosphatase PTP, which is a deactivator of ERK. We next show how these network motifs and a particular geometry of a neuron control the cAMP concentration gradients and cAMP-induced signalling. In hippocampal neurons the cell body and dendrites have the same surface density of β-ARs, generating similar adenylyl cyclase activities and cAMP levels near both the soma and dendrite surfaces [37]. Assuming that PDE4 has a high Michaelis constant, the distance over which steady-state cAMP gradients decay (L_{grad}) is determined by the ratio of the cAMP diffusivity (D) to phosphodiesterase activity (k_{deact}) and is given by Eq. (1) [9]. This equation yields the gradient decay length of approximately 4 μm that can decrease to about 2.5 μm, when PKA feedback activates PDE4 [6]. The neuron soma and dendrites have very different geometries. The soma has the diameter of about 20–30 μm, whereas a dendrite has the much smaller diameter of 1–3 μm. Therefore, in the neuronal soma, the cAMP concentration progressively decays with the distance from the membrane, whereas cAMP can remain high in the dendrites because of their small diameters.

How does the cAMP concentration profile influence the downstream ERK activation? PKA is the immediate downstream target of cAMP, and the cAMP gradients induce spatially restricted PKA activity. The PKA–phosphodiesterase negative feedback loop makes gradients of cAMP and PKA activity more precipitous and locally confined. Although PKA activates B-Raf, computer simulations show that the steady-state spatial distribution of PKA-induced B-Raf and MEK activities are almost uniform, which is explained by robust B-Raf activation kinetic parameters [37]. The lack of spatial gradients is also confirmed experimentally for MEK [37]. However, ERK activity is found to be spatially heterogeneous; dually phosphorylated, active ERK forms spatial domains that bear a resemblance to the cAMP concentration domains. These, at first glance contradictory, observations are explained by the fact that the spatial heterogeneity of cAMP and PKA activity profiles is transmitted downstream of the PKA/ERK cascade by the feedforward motif where PKA not only activates B-Raf, but also inhibits the ERK phosphatase PTP. Within a certain range of kinetic parameters this feedforward motif operates as a logical AND gate where appreciable activation of ERK requires both activation of MEK and inhibition of PTP. In other words, only in concord with PKA-induced inhibition of PTP, spatially homogeneous active MEK can switch on ERK activity. This restricts ERK stimulation to spatial domains that have high PKA activity. Thus, both the proper interaction design and appropriate reaction kinetics are necessary to enable signalling cascades to generate precise, complex spatial guidance for downstream effector processes.

5.3. Cell polarization and spatial signalling

Cell polarization is a process of crucial importance for chemotaxis of eukaryotic cells. During chemotaxis, cell migrate in response to gradients of the concentrations of extracellular chemoattractants [40]. Polarization is linked to the spatial symmetry breaking, when the homogeneous distribution of specific signalling components is replaced by their persistent localization to opposite ends of the cell. Although multiple hypotheses have been proposed in the theoretical studies of cell polarization, a quantitative understanding of experimentally observed phenomena is still lacking. Current models explain the occurrence of cell polarization by bistability of a reaction network, coupled with diffusion and brought about by a strong positive feedback loop or a double negative feedback loop (reviewed in Ref. [41]).

6. Long-range signalling, retrograde transport and phosphoprotein waves

How survival signals propagate along neuronal axons to the soma over very long distances has puzzled neurobiologists for many years. The survival and function of developing or damaged neurons depends on neurotrophins, such as the nerve growth factor (NGF) that is generated by peripheral tissues. NGF binds to its receptor, TrkA, on distal axons, which induces survival signalling to be transmitted to the neuron body, located up to one meter away. Obviously, diffusion is ruled out as a mechanism for such signalling, since diffusion would be prohibitively slow. According to a widely accepted model, shortly after NGF binding to TrkA at nerve terminals, the NGF–TrkA complexes are internalized into endosomes by clathrin-mediated endocytosis. Signalling endosomes containing activated TrkA with associated NGF are retrogradely transported to the cell bodies [42]. This retrograde transport is critical for neuronal survival. However, experiments on compartmented cultures show that survival signals can also be transmitted by NGF-independent mechanisms [43]. In fact, it was recently demonstrated that following nerve injury at distal axon, phosphorylated kinases, such as ERK1/2, translocate to the soma within a signalling complex, which contains intermediate filament vimentin, importins and the molecular motor dynein [44]. The binding of vimentin to phosphorylated ERK was shown to protect the phosphotyrosine residues on ERK against the phosphatase activity, thus maintaining ERK in the active state [45].

Experiments on compartmented cultures showed that after stimulation of distal axons with NGF, tyrosine phosphorylation is detected in neuron bodies, located centimetres away from the point of NGF application, as early as in 10–15 min [43]. With a rate of molecular motors of about 1–10 μm/min, measurable phosphorylation signal carried out by the retrograde transport over the distance of 10 cm would be detected in 2.8–28 h. Therefore, although transport of endosomes containing the NGF–TrkA complexes and phosphorylated kinases driven by molecular motors are robust mechanisms of retrograde signalling, they cannot account for the observed initial burst of tyrosine phosphorylation in the neuron soma. A lateral propagation of TrkA activation [46] should also be excluded, since nearly complete inhibition of TrkA in the cell bodies and proximal axons did not affect survival, whereas TrkA inhibition at distal axons induced apoptosis [47]. I propose that the initial survival signals are transmitted by waves of protein phosphorylation emerging from kinase/phosphatase cascades, such as MAPK or PI3K cascades, or GEF/GAP cascades of G-protein activation [48].

7. Outlook and future directions

Two principally different physico-chemical scenarios were proposed to account for the generation of positional information, which guides diverse physiological processes. The first is the Turing mechanism of the symmetry breaking in a *homogeneous reaction–diffusion* system, which leads to the formation of periodic spatial patterns of species concentrations [7]. A distinctive feature of the second mechanism proposed by Brown and Kholodenko to operate within living cells is the *initial heterogeneity* due to the spatial separation of an activation reaction and deactivation reaction for a target protein [9]. The intracellular gradients generated by this mechanism are then converted into a large variety of heterogeneous steady-state concentration patterns [4]. For instance, a signalling cascade can generate the effective stratification of the space between the cell membrane and the nucleus into concentric layers (Fig. 2B). The kinase activity of each cascade level is almost constant between the plasma membrane and the border of the corresponding layer where the activity abruptly decays [31]. Arbitrary spatial concentration patterns can be generated in signalling networks where the spatial segregation of opposing reactions is combined with feedforward and feedback loops [21,37]. The aspects of complicated spatial activity patterns, which were briefly discussed for GTPase networks, imply that GTPase networks may serve as devices for spatial computation inside living cells [21]. Importantly, if the diffusivities of an active (e.g., phosphorylated) form and inactive (unphosphorylated) form differ, not only do these forms generate non-uniform spatial profiles, but the gradients of the total protein abundance emerge within a cell (Fig. 1).

Further work is required to quantitatively understand spatially distributed cell signalling. To comprehend the physiological regulation, the control exerted by variations in cell size and shape, network architecture, kinetic parameters, and diffusion on the signal propagation and spatial concentration patterns should be precisely quantified [32]. Similar to the principles established for spatially homogeneous networks [49], we can expect that the control over salient features of the spatiotemporal dynamics is not exerted by single negative or positive regulators. Rather, the control is distributed between multiple processes, including spatially segregated activators and deactivators, feedback and feedforward motifs, diffusion, and cell size [37,50]. The spatiotemporal behaviour of cellular networks creates a code of biochemical and biological specificity of cellular responses.

Acknowledgement

References

[1] Kholodenko, B.N. and Westerhoff, H.V. (1995) The macroworld versus the microworld of biochemical regulation and control. Trends Biochem. Sci. 20, 52–54.

[2] Agius, L., Sheratt, H.S.A. (1997) Channeling in Intermediary Metabolism. Portland Press.

[3] Srere, P.A. (2000) Macromolecular interactions: tracing the roots. Trends Biochem. Sci. 25, 150–153.

[4] Bastiaens, P., Caudron, M., Niethammer, P. and Karsenti, E. (2006) Gradients in the self-organization of the mitotic spindle. Trends Cell Biol. 16, 125–134.

[5] Mori, Y., Jilkine, A. and Edelstein-Keshet, L. (2008) Wave-pinning and cell polarity from a bistable reaction–diffusion system. Biophys. J. 94, 3684–3697.

[6] Kholodenko, B.N. and Kolch, W. (2008) Giving space to cell signaling. Cell 133, 566–567.

[7] Turing, A.M. (1952) The chemical basis of morphogenesis. Phil. Trans. R. Soc. Lond. B Biol. Sci. 237, 37–72.

[8] Asai, R., Taguchi, E., Kume, Y., Saito, M. and Kondo, S. (1999) Zebrafish leopard gene as a component of the putative reaction–diffusion system. Mech. Dev. 89, 87–92.

[9] Brown, G.C. and Kholodenko, B.N. (1999) Spatial gradients of cellular phospho-proteins. FEBS Lett. 457, 452–454.

[10] Seet, B.T., Dikic, I., Zhou, M.M. and Pawson, T. (2006) Reading protein modifications with interaction domains. Nat. Rev. Mol. Cell Biol. 7, 473–483.

[11] Sauro, H.M. and Kholodenko, B.N. (2004) Quantitative analysis of signaling networks. Prog. Biophys. Mol. Biol. 86, 5–43.

[12] Goldbeter, A. and Koshland Jr., D.E. (1984) Ultrasensitivity in biochemical systems controlled by covalent modification. Interplay between zero-order and multistep effects. J. Biol. Chem. 259, 14441–14447.

[13] Bluthgen, N., Bruggeman, F.J., Legewie, S., Herzel, H., Westerhoff, H.V. and Kholodenko, B.N. (2006) Effects of sequestration on signal transduction cascades. FEBS J. 273, 895–906.

[14] van Albada, S.B. and ten Wolde, P.R. (2007) Enzyme localization can drastically affect signal amplification in signal transduction pathways. PLoS Comput. Biol. 3, 1925–1934.

[15] Kalab, P., Weis, K. and Heald, R. (2002) Visualization of a Ran-GTP gradient in interphase and mitotic Xenopus egg extracts. Science 295, 2452–2456.

[16] Niethammer, P., Bastiaens, P. and Karsenti, E. (2004) Stathmin–tubulin interaction gradients in motile and mitotic cells. Science 303, 1862–1866.

[17] Maeder, C.I., Hink, M.A., Kinkhabwala, A., Mayr, R., Bastiaens, P.I. and Knop, M. (2007) Spatial regulation of Fus3 MAP kinase activity through a reaction–diffusion mechanism in yeast pheromone signalling. Nat. Cell Biol. 9, 1319–1326.

[18] Fuller, B.G. et al. (2008) Midzone activation of aurora B in anaphase produces an intracellular phosphorylation gradient. Nature 453, 1132–1136.

[19] Slepchenko, B.M. and Terasaki, M. (2003) Cyclin aggregation and robustness of bio-switching. Mol. Biol. Cell 14, 4695–4706.

[20] Wagner, J. and Keizer, J. (1994) Effects of rapid buffers on Ca^{2+} diffusion and Ca^{2+} oscillations. Biophys. J. 67, 447–456.

[21] Stelling, J. and Kholodenko, B.N. (2008) Signaling cascades as cellular devices for spatial computations. J. Math. Biol.

[22] Kusumi, A. et al. (2005) Paradigm shift of the plasma membrane concept from the two-dimensional continuum fluid to the partitioned fluid: high-speed single-molecule tracking of membrane molecules. Annu. Rev. Biophys. Biomol. Struct. 34, 351–378.

[23] Singer, S.J. and Nicolson, G.L. (1972) The fluid mosaic model of the structure of cell membranes. Science 175, 720–731.

[24] Ritchie, K., Shan, X.Y., Kondo, J., Iwasawa, K., Fujiwara, T. and Kusumi, A. (2005) Detection of non-Brownian diffusion in the cell membrane in single molecule tracking. Biophys. J. 88, 2266–2277.

[25] Mayawala, K., Vlachos, D.G. and Edwards, J.S. (2006) Spatial modeling of dimerization reaction dynamics in the plasma membrane: Monte Carlo vs. Continuum differential equations. Biophys. Chem. 121, 194–208.

[26] Brinkerhoff, C.J., Choi, J.S. and Linderman, J.J. (2008) Diffusion-limited reactions in G-protein activation: unexpected consequences of antagonist and agonist competition. J. Theor. Biol. 251, 561–569.

[27] Niehaus, A.M., Vlachos, D.G., Edwards, J.S., Plechac, P. and Tribe, R. (2008) Microscopic simulation of membrane molecule diffusion on corralled membrane surfaces. Biophys. J. 94, 1551–1564.

[28] Costa, M.N., Radhakrishnan, K., Wilson, B.S., Vlachos, D.G. and Edwards, J.S. (2009) Coupled stochastic spatial and non-spatial simulations of ErbB1 signaling pathways demonstrate the importance of spatial organization in signal transduction. PLoS One 4, e6316.

[29] Berezhkovskii, A.M., Coppey, M. and Shvartsman, S.Y. (2009) Signaling gradients in cascades of two-state reaction–diffusion systems. Proc. Natl. Acad. Sci. USA 106, 1087–1092.

[30] Kholodenko, B.N. (2002) MAP kinase cascade signaling and endocytic trafficking: a marriage of convenience? Trends Cell Biol. 12, 173–177.

[31] Munoz-Garcia, J., Neufeld, Z. and Kholodenko, B.N. (2009) Positional information generated by spatially distributed signaling cascades. PLoS Comput. Biol. 5, e1000330.

[32] Kholodenko, B.N. (2006) Cell-signalling dynamics in time and space. Nat. Rev. Mol. Cell. Biol. 7, 165–176.

[33] Jilkine, A., Maree, A.F. and Edelstein-Keshet, L. (2007) Mathematical model for spatial segregation of the Rho-family GTPases based on inhibitory crosstalk. Bull. Math. Biol. 69, 1943–1978.

[34] Athale, C.A., Dinarina, A., Mora-Coral, M., Pugieux, C., Nedelec, F. and Karsenti, E. (2008) Regulation of microtubule dynamics by reaction cascades around chromosomes. Science 322, 1243–1247.

[35] Meyers, J., Craig, J. and Odde, D.J. (2006) Potential for Control of Signaling Pathways via Cell Size and Shape. Curr. Biol. 16, 1685–1693.

[36] Nalbant, P., Hodgson, L., Kraynov, V., Toutchkine, A. and Hahn, K.M. (2004) Activation of endogenous Cdc42 visualized in living cells. Science 305, 1615–1619.

[37] Neves, S.R. et al. (2008) Cell shape and negative links in regulatory motifs together control spatial information flow in signaling networks. Cell 133, 666–680.

[38] Fell, D.A. (1980) Theoretical analyses of the functioning of the high- and low-Km cyclic nucleotide phosphodiesterases in the regulation of the concentration of adenosine 3',5'-cyclic monophosphate in animal cells. J. Theor. Biol. 84, 361–385.

[39] Zaccolo, M. and Pozzan, T. (2002) Discrete microdomains with high concentration of cAMP in stimulated rat neonatal cardiac myocytes. Science 295, 1711–1715.

[40] Parent, C.A. and Devreotes, P.N. (1999) A cell's sense of direction. Science 284, 765–770.

[41] Iglesias, P.A. and Devreotes, P.N. (2008) Navigating through models of chemotaxis. Curr. Opin. Cell Biol. 20, 35–40.

[42] Ginty, D.D. and Segal, R.A. (2002) Retrograde neurotrophin signaling: Trk-ing along the axon. Curr. Opin. Neurobiol. 12, 268–274.

[43] Campenot, R.B. and MacInnis, B.L. (2004) Retrograde transport of neurotrophins: fact and function. J. Neurobiol. 58, 217–229.

[44] Perlson, E., Hanz, S., Ben-Yaakov, K., Segal-Ruder, Y., Seger, R. and Fainzilber, M. (2005) Vimentin-dependent spatial translocation of an activated MAP kinase in injured nerve. Neuron 45, 715–726.

[45] Perlson, E., Michaelevski, I., Kowalsman, N., Ben-Yaakov, K., Shaked, M., Seger, R., Eisenstein, M. and Fainzilber, M. (2006) Vimentin binding to phosphorylated Erk sterically hinders enzymatic dephosphorylation of the kinase. J. Mol. Biol. 364, 938–944.

[46] Reynolds, A.R., Tischer, C., Verveer, P.J., Rocks, O. and Bastiaens, P.I. (2003) EGFR activation coupled to inhibition of tyrosine phosphatases causes lateral signal propagation. Nat. Cell. Biol. 5, 447–453.

[47] MacInnis, B.L., Senger, D.L. and Campenot, R.B. (2003) Spatial requirements for TrkA kinase activity in the support of neuronal survival and axon growth in rat sympathetic neurons. Neuropharmacology 45, 995–1010.

[48] Markevich, N.I., Tsyganov, M.A., Hoek, J.B. and Kholodenko, B.N. (2006) Long-range signaling by phosphoprotein waves arising from bistability in protein kinase cascades. Mol. Syst. Biol. 2, 61.

[49] Brown, G.C., Westerhoff, H.V. and Kholodenko, B.N. (1996) Molecular control analysis: control within proteins and molecular processes. J. Theor. Biol. 182, 389–396.

[50] Peletier, M.A., Westerhoff, H.V. and Kholodenko, B.N. (2003) Control of spatially heterogeneous and time-varying cellular reaction networks: a new summation law. J. Theor. Biol. 225, 477–487.